

Constraints on interacting dark energy models from the DESI BAO and DES supernovae data

Tian-Nuo Li,¹ Peng-Ju Wu,¹ Guo-Hong Du,¹ Shang-Jie Jin,^{1,2} Hai-Li Li,³ Jing-Fei Zhang,^{1,*} and Xin Zhang^{1,4,5,†}

¹*Key Laboratory of Cosmology and Astrophysics (Liaoning Province) & Department of Physics, College of Sciences, Northeastern University, Shenyang 110819, China*

²*Department of Physics, University of Western Australia, Perth WA 6009, Australia*

³*Basic Teaching Department, Shenyang Institute of Engineering, Shenyang 110136, China*

⁴*Key Laboratory of Data Analytics and Optimization for Smart Industry (Ministry of Education), Northeastern University, Shenyang 110819, China*

⁵*National Frontiers Science Center for Industrial Intelligence and Systems Optimization, Northeastern University, Shenyang 110819, China*

The recent results from the first year baryon acoustic oscillations (BAO) data released by the Dark Energy Spectroscopic Instrument (DESI), combined with cosmic microwave background (CMB) and type Ia supernova (SN) data, have shown a detection of significant deviation from a cosmological constant for dark energy. In this work, we utilize the latest DESI BAO data in combination with the SN data from the full five-year observations of the Dark Energy Survey and the CMB data from the Planck satellite to explore potential interactions between dark energy and dark matter. We consider four typical forms of the interaction term Q . Our findings suggest that interacting dark energy (IDE) models with $Q \propto \rho_{de}$ support the presence of an interaction where dark energy decays into dark matter. Specifically, the deviation from ΛCDM for the IDE model with $Q = \beta H_0 \rho_{de}$ reaches the 3σ level. These models yield a lower value of Akaike information criterion than the ΛCDM model, indicating a preference for these IDE models based on the current observational data. For IDE models with $Q \propto \rho_c$, the existence of interaction depends on the form of the proportionality coefficient Γ . The IDE model with $Q = \beta H \rho_c$ yields $\beta = 0.0003 \pm 0.0011$, which essentially does not support the presence of the interaction. In general, whether the observational data support the existence of interaction is closely related to the model. Our analysis helps to elucidate which type of IDE model can better explain the current observational data.

I. INTRODUCTION

In 1998, two independent studies of distant type Ia supernovae (SN) discovered the accelerated expansion of the universe [1, 2], which was further independently confirmed by observations of the cosmic microwave background (CMB) [3–5] and baryon acoustic oscillations (BAO) [6–8]. In order to explain the cosmic acceleration, the concept of “dark energy”, which is an exotic form of energy with negative pressure, has been proposed. At present, dark energy occupies about 68% of the total energy density of the cosmos, dominating the evolution of the current universe. The cosmological constant Λ , proposed by Einstein in 1917, has been regarded as the most straightforward candidate for dark energy up to now. For a long time, the ΛCDM model, which is primarily composed of a cosmological constant Λ and cold dark matter (CDM), has been considered a standard model of cosmology.

The ΛCDM model fits the CMB data quite well, and the six basic parameters have been constrained with unprecedented precision. However, with the measurement precisions of the cosmological parameters improved, some

puzzling issues appeared. Especially for the measurement of the Hubble constant, the local distance ladder method gives $H_0 = 73.04 \pm 1.04 \text{ km s}^{-1} \text{ Mpc}^{-1}$ [9], while the CMB observation infers $H_0 = 67.36 \pm 0.54 \text{ km s}^{-1} \text{ Mpc}^{-1}$ [5], revealing a tension above 5σ . Recently, the Hubble tension has been widely discussed in the literature [10–23] (see also e.g., Refs. [24–42] for some forecast analyses). On the other hand, the cosmological constant Λ in the ΛCDM model, which is equivalent to the vacuum energy density, also has been suffering from serious theoretical challenges, namely, the “fine-tuning” and “cosmic coincidence” problems [43, 44]. Therefore, it is far-fetched to take the ΛCDM model as the eventual cosmological scenario. All of these facts imply that we need to consider new physics beyond the standard ΛCDM model.

Among the different extensions to the ΛCDM model, there exists a category known as interacting dark energy (IDE) models, in which the direct and nongravitational interaction between dark energy and dark matter is considered. Some studies about IDE models have also been conducted in Refs. [45–68]. The IDE models not only can help alleviate the Hubble tension [16, 69, 70] and the coincidence problem of dark energy [71–73] but also can help probe the fundamental nature of dark energy and dark matter. In fact, the CMB data alone can only measure the six basic parameters at high precision for the ΛCDM model, and when the model is extended to include new parameters, the CMB data alone cannot provide precise measurements for them. This is because the newly ex-

* Corresponding author.
jfzhang@mail.neu.edu.cn

† Corresponding author.
zhangxin@mail.neu.edu.cn

tended parameters beyond the Λ CDM model will severely degenerate with other parameters. Hence, low-redshift cosmological probes such as the BAO and SN observation, need to be combined with the CMB data to break the cosmological parameter degeneracies.

Recently, the Dark Energy Spectroscopic Instrument (DESI) collaboration released the first year data from the measurements of BAO in galaxy, quasar, and Lyman- α (Ly α) forest tracers [74, 75], and the cosmological parameter results derived from these measurements [76]. For the cosmological constraints, DESI collaboration provided cosmological inference results for various cosmological models, including the Λ CDM model, the w CDM model, and the w_0w_a CDM model. In particular, for the w_0w_a CDM model, combining the DESI BAO data with the CMB data and DESY5 data leads to deviations from Λ CDM at up to 3.9σ . Interestingly, Park *et al.* [77] have also reported similar evidence for dynamical dark energy using the w_0w_a CDM model with other BAO data. The deviations from the Λ CDM model observed in the DESI BAO data have sparked extensive discussions regarding dark energy. Recently, several studies have sought to constrain various aspects of cosmological physics using the DESI BAO data [78–90].

Besides, the DESI data along with other data like CMB and type Ia supernovae have been considered to constrain the IDE model [91]. However, in the study of IDE models, the choice of different forms of interaction terms affects the results. Hence, in this work, we use the current observational data including the DESI BAO data, the CMB data from Planck, and the SN data from Dark Energy Survey (DES), to constrain IDE models by considering four typical forms of interaction term Q . Our motivation is to explore whether there is an interaction between dark energy and dark matter and which types of IDE models are more supported by the current cosmological observations.

This work is organized as follows. In Sec. II, we briefly introduce the IDE models and cosmological data used in this work. In Sec. III, we report the constraint results and make some relevant discussions. The conclusion is given in Sec. IV.

II. MODELS AND DATA

A. Interacting dark energy models

In a flat Friedmann–Roberston–Walker universe, the Friedmann equation is given by

$$3M_{\text{pl}}^2 H^2 = \rho_{\text{de}} + \rho_c + \rho_b + \rho_r, \quad (1)$$

where $3M_{\text{pl}}^2 H^2$ is the critical density of the universe, and ρ_{de} , ρ_c , ρ_b , and ρ_r represent the energy densities of dark energy, cold dark matter, baryon, and radiation, respectively. In the IDE models, if assuming a direct interaction between dark energy and cold dark matter, the

energy conservation equations can be given by

$$\dot{\rho}_{\text{de}} + 3H(1+w)\rho_{\text{de}} = Q, \quad (2)$$

$$\dot{\rho}_c + 3H\rho_c = -Q, \quad (3)$$

where the dot is the derivative with respect to the cosmic time t , H is the Hubble parameter, w is the equation of state of dark energy, and Q denotes the phenomenological interaction term describing the energy transfer rate between dark energy and dark matter due to the interaction. The form of Q is usually assumed to be proportional to the energy density of dark energy or cold dark matter [92, 93]. The proportionality coefficient Γ has the dimension of energy, and so it is with the form of $\Gamma = \beta H$ or $\Gamma = \beta H_0$, where β is the dimensionless coupling parameter. $\beta > 0$ indicates cold dark matter decaying into dark energy, $\beta < 0$ indicates dark energy decaying into cold dark matter, and $\beta = 0$ indicates no interaction between dark energy and cold dark matter. In this work, we do not aim to study the nature of dark energy purely from a theoretical perspective but instead approach the issue of dark energy phenomenologically. We focus solely on the case where $w = -1$ to avoid introducing additional parameters, and the corresponding IDE model is denoted as the I Λ CDM model. Hence, we consider four typical phenomenological forms of Q , i.e., $Q = \beta H\rho_{\text{de}}$ (I Λ CDM1), $Q = \beta H\rho_c$ (I Λ CDM2), $Q = \beta H_0\rho_{\text{de}}$ (I Λ CDM3), and $Q = \beta H_0\rho_c$ (I Λ CDM4), on I Λ CDM models.

In recent years, it has been found that IDE models may experience an early-time large-scale instability problem [94, 95]. This instability arises because cosmological perturbations of dark energy within IDE models diverge in certain regions of parameter space, potentially leading to the breakdown of IDE cosmology at the perturbation level. To avoid this problem, the parameterized post-Friedmann (PPF) approach [96, 97] was extended to the IDE models [98–101], referred to as the ePPF approach. This ePPF approach can safely calculate the cosmological perturbations in the whole parameter space of the IDE models. In this work, we employ the ePPF approach to treat the cosmological perturbations; see e.g. Refs. [55, 102] for the application of the ePPF approach.

B. Cosmological data

In this work, we employ the Markov-chain Monte Carlo (MCMC) package `CosmoMC` to infer the posterior distributions of parameters [103, 104]. We assess the convergence of the MCMC chains using the Gelman-Rubin statistics quantity $R - 1 < 0.02$ [105]. The MCMC chains are analyzed using the public package `Getdist` [106]. The basic parameter space of the IDE models is $\{\Omega_b h^2, \Omega_c h^2, \log(10^{10} A_s), 100\theta_{\text{MC}}, n_s, \tau_{\text{reio}}, \beta\}$. We use the current observational data to constrain the IDE models and obtain the best-fit values and the $1-2\sigma$ confidence level ranges for the parameters of interest $\{H_0, \Omega_m, \beta\}$. We adopt the following observational datasets:

TABLE I. Statistics of the DESI samples utilized in the DESI DR1 BAO measurements for this paper.

Tracer	Redshift	z_{eff}	D_M/r_d	D_H/r_d	D_V/r_d
BGS	0.1 – 0.4	0.30	—	—	7.93 ± 0.15
LRG1	0.4 – 0.6	0.51	13.62 ± 0.25	20.98 ± 0.61	—
LRG2	0.6 – 0.8	0.71	16.85 ± 0.32	20.08 ± 0.60	—
LRG3+ELG1	0.8 – 1.1	0.93	21.71 ± 0.28	17.88 ± 0.35	—
ELG2	1.1 – 1.6	1.32	27.79 ± 0.69	13.82 ± 0.42	—
QSO	0.8 – 2.1	1.49	—	—	26.07 ± 0.67
Lya QSO	1.77 – 4.16	2.33	39.71 ± 0.94	8.52 ± 0.17	—

• Cosmic Microwave Background. The Planck satellite has provided precise measurements of the power spectra of anisotropies in the CMB [5, 107]. These observations hold significant importance for cosmology as they have revealed details about the matter composition, topology, and large-scale structure of the universe. We adopt the Planck TT, TE, EE spectra at $\ell \geq 30$, the low- ℓ temperature Commander likelihood, and the low- ℓ SimAll EE likelihood from the Planck 2018 data release [5].¹ We also employ conservatively the Planck PR4 lensing likelihood from combination of NPIPE PR4 Planck CMB lensing reconstruction [108].² We label the Planck 2018 dataset and the Planck PR4 lensing dataset as CMB.

• Baryon Acoustic Oscillations. BAO provides a standard ruler for a typical length scale to measure the angular diameter distance $D_A(z)$ and Hubble parameter $H(z)$. BAO can be measured by analyzing the spatial distribution of galaxies and consequently provides an independent way to measure the expansion rate of the universe and can impose significant constraints on the cosmological parameters [8, 109–111]. The DESI BAO data include tracers of the bright galaxy sample (BGS), luminous red galaxies (LRG), emission line galaxies (ELG), quasars (QSO), and the Ly α forest in a redshift range $0.1 \leq z \leq 4.2$ [74, 75]. These tracers are described through the transverse comoving distance D_M/r_d , the angle-averaged distance D_V/r_d , and the Hubble horizon D_H/r_d , where r_d is the comoving sound horizon at the drag epoch. We use 12 DESI BAO measurements in Table I based on Ref. [76].³ We label the DESI BAO data as DESI.

• Type Ia Supernovae. SNe provide measurements of luminosity distances $D_L(z) = (1+z)D_M(z)$. The luminosity distances are powerful distance indicators to probe the background evolution of the universe, especially, the equation of state of dark energy. Recently,

the DES collaboration released part of the full 5-year data based on a new, homogeneously selected sample of 1635 photometrically-classified supernovae (with redshifts in the range $0.1 < z < 1.3$), complemented by 194 low-redshift supernovae (with redshifts in the range $0.025 < z < 0.1$), totaling 1829 supernovae. This sample quintuples the number of high-quality $z > 0.5$ SNe compared to the previous leading Pantheon+ compilation, and results in the tightest cosmological constraints achieved by any supernova data set to date [112]. We label the SN data as DESY5.⁴

III. RESULTS AND DISCUSSIONS

In this section, we shall report the constraint results of the cosmological parameters. We consider the Λ CDM1 ($Q = \beta H \rho_{de}$), Λ CDM2 ($Q = \beta H \rho_c$), Λ CDM3 ($Q = \beta H_0 \rho_{de}$), and Λ CDM4 ($Q = \beta H_0 \rho_c$) models to perform a cosmological analysis using current observational data, including DESI, CMB, and DESY5 data. We show the 1σ and 2σ posterior distribution contours for various cosmological parameters in the four IDE models, as shown in Figs. 1–3. The 1σ errors for the marginalized parameter constraints are summarized in Table II. We compare the best-fit predictions for the three different types of (rescaled) distances obtained by DESI BAO measurements using CMB+DESI data in the Λ CDM, Λ CDM1, and Λ CDM2 models, as shown in Fig. 4.

In Fig. 1, we show the constraint results of the CMB data in the $\beta-H_0$ (left panel) and $\beta-\Omega_m$ (right panel) planes for the four IDE models. When using the CMB data alone, the constraint values of β are $-0.13^{+0.55}_{-0.36}$ (Λ CDM1), -0.0018 ± 0.0022 (Λ CDM2), $-0.15^{+0.74}_{-0.39}$ (Λ CDM3), and $-0.13^{+0.15}_{-0.13}$ (Λ CDM4). We can find that Λ CDM2 gives the best constraints on the parameter β , followed by Λ CDM4, while Λ CDM1 and Λ CDM3 give comparable constraint results. This is because in the early universe, both H and ρ_c have relatively high values, leading to that β must be very small and can be

¹ The likelihood is available from <https://pla.esac.esa.int>.

² The likelihood is available from https://github.com/carronj/planck_PR4_lensing.

³ The DESI BAO data used in this work has been made public along the Data Release 1 (details in <https://data.desi.lbl.gov/doc/releases/>).

⁴ Data available at <https://github.com/des-science/DES-SN5YR>.

TABLE II. Fitting results (68.3% confidence level) in the Λ CDM and IDE models from the CMB, CMB+DESI, and CMB+DESI+DESY5 data. Here, H_0 is in units of $\text{km s}^{-1} \text{Mpc}^{-1}$.

Data	Parameter	Λ CDM	IACDM1	IACDM2	IACDM3	IACDM4
CMB	H_0	67.28 ± 0.52	$66.1^{+5.1}_{-4.0}$	65.9 ± 1.5	$66.2^{+3.5}_{-3.1}$	64.4 ± 3.2
	Ω_m	0.3158 ± 0.0072	$0.35^{+0.13}_{-0.16}$	$0.333^{+0.020}_{-0.022}$	$0.35^{+0.12}_{-0.15}$	$0.388^{+0.055}_{-0.091}$
	β	—	$-0.13^{+0.55}_{-0.36}$	-0.0018 ± 0.0022	$-0.15^{+0.74}_{-0.39}$	$-0.10^{+0.15}_{-0.13}$
CMB+DESI	H_0	68.05 ± 0.4	$70.5^{+1.5}_{-1.8}$	68.72 ± 0.61	70.4 ± 1.8	69.4 ± 1.0
	Ω_m	0.305 ± 0.0052	$0.219^{+0.061}_{-0.050}$	0.2976 ± 0.0073	0.208 ± 0.075	$0.279^{+0.017}_{-0.020}$
	β	—	0.29 ± 0.18	0.0011 ± 0.0013	$0.36^{+0.37}_{-0.28}$	0.075 ± 0.052
CMB+DESI+DESY5	H_0	67.60 ± 0.37	66.18 ± 0.63	67.72 ± 0.56	65.94 ± 0.63	66.59 ± 0.69
	Ω_m	0.3113 ± 0.005	0.367 ± 0.020	0.310 ± 0.0069	0.393 ± 0.026	0.335 ± 0.015
	β	—	-0.197 ± 0.071	0.0003 ± 0.0011	-0.40 ± 0.13	-0.067 ± 0.038
	χ^2_{\min}	2246.853	2242.266	2246.172	2240.719	2244.764
$\Delta \text{ AIC}$		0	-2.627	1.319	-4.134	-0.089

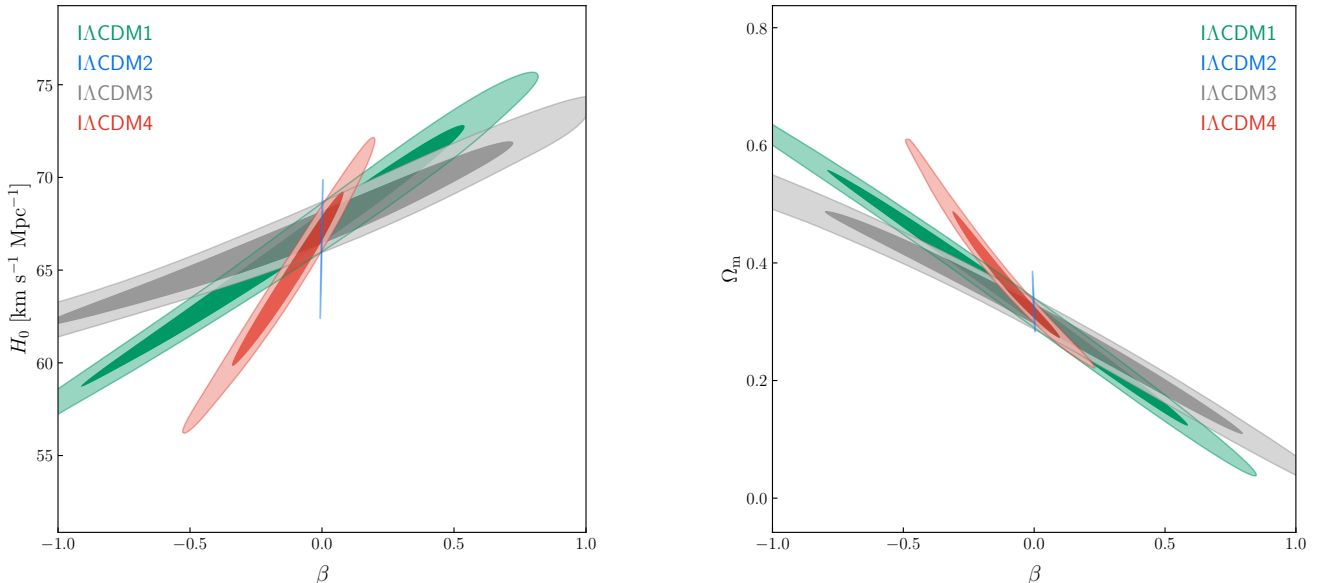


FIG. 1. Two-dimensional marginalized contours (68.3% and 95.4% confidence level) in the β – H_0 and β – Ω_m planes by using the CMB data in the IACDM1, IACDM2, IACDM3, and IACDM4 models.

constrained tightly. Therefore, in the IACDM2 model, as a probe of the early universe, CMB data can provide relatively stringent constraints on β . Furthermore, we investigate the impact of including PR4 lensing data on parameter constraints. Our results show that in the Λ CDM model, CMB data (adding PR4 lensing data to the Planck 2018 data) results in $\sigma(H_0) = 0.52 \text{ km s}^{-1} \text{ Mpc}^{-1}$ and $\sigma(\Omega_m) = 0.0072$, which are 14.7% and 15.2% better than those of Planck 2018 data [60], respectively. However, in the IDE models, the addition of PR4 lensing data only slightly improves the parameter constraints.

In Fig. 2, we show the constraint results of the

CMB+DESI data in the β – H_0 (left panel) and β – Ω_m (right panel) planes for the four IDE models. The constraint values of β are 0.29 ± 0.18 (IACDM1), 0.0011 ± 0.0013 (IACDM2), $0.36^{+0.37}_{-0.28}$ (IACDM3), and 0.075 ± 0.052 (IACDM4). We find that the combinations including DESI data tend to favor slightly higher values of H_0 and lower values of Ω_m compared to the central values derived from the CMB data. In this case, β is positively correlated with H_0 , as clearly seen in the left panel of Fig. 2, thus resulting in higher central values of β . Higher positive values of β further support the scenario where cold dark matter decays into dark energy.

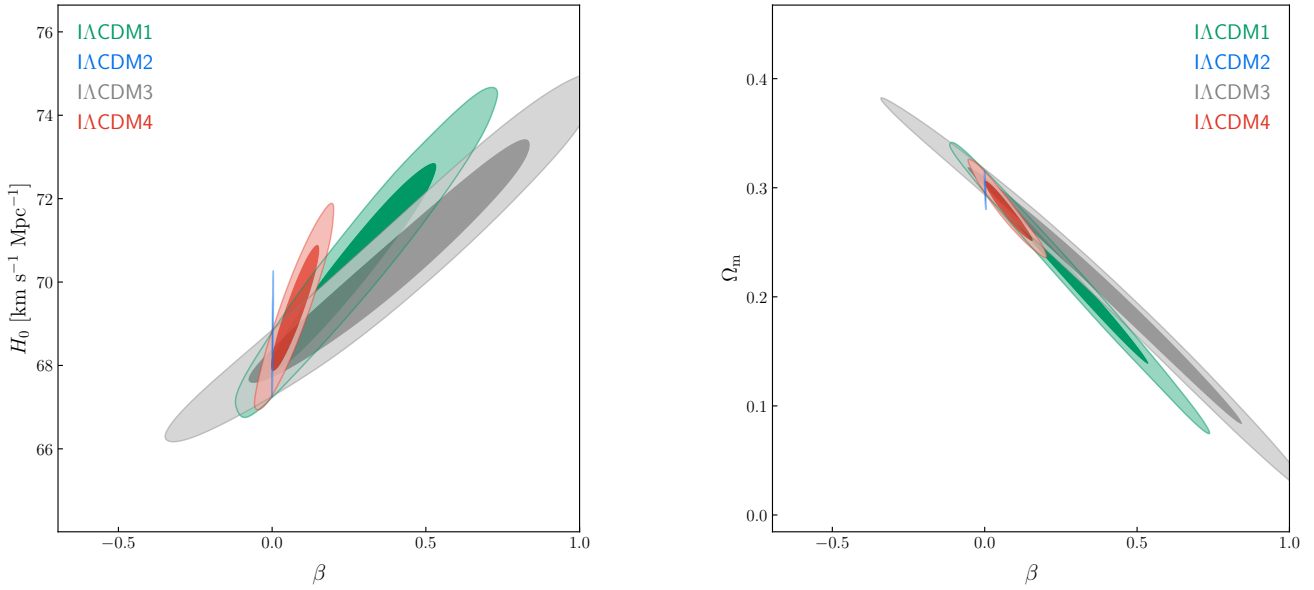


FIG. 2. Two-dimensional marginalized contours (68.3% and 95.4% confidence level) in the β - H_0 and β - Ω_m planes by using the CMB+DESI data in the IACDM1, IACDM2, IACDM3, and IACDM4 models.

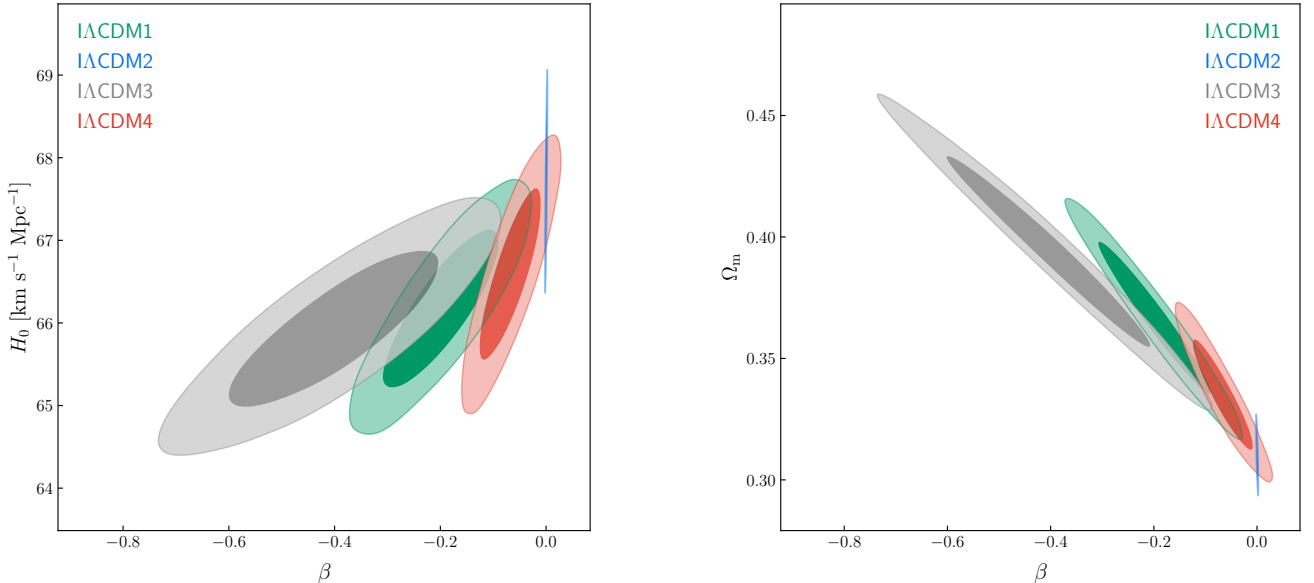


FIG. 3. Two-dimensional marginalized contours (68.3% and 95.4% confidence level) in the β - H_0 and β - Ω_m planes by using the CMB+DESI+DESY5 data in the IACDM1, IACDM2, IACDM3, and IACDM4 models.

For instance, the IACDM1 model with $\beta = 0.29 \pm 0.18$ provides supporting evidence for an interaction, and the deviation of β from the standard Λ CDM model reaches 1.6σ . Conversely, in the IACDM2 model, the value of β being close to zero indicates no interaction between dark energy and cold dark matter.

In Fig. 3, we show the constraint results of the CMB+DESI+DESY5 data in the β - H_0 (left panel)

and β - Ω_m (right panel) planes for the four IDE models. The combination of low-redshift data and CMB data can effectively break the cosmological parameter degeneracies. For example, in the IACDM2 model, CMB+DESI+DESY5 results in $\sigma(\beta) = 0.0011$, $\sigma(H_0) = 0.56$ km s $^{-1}$ Mpc $^{-1}$, and $\sigma(\Omega_m) = 0.0069$, which are 50%, 62.6%, and 67.1% better than those of CMB, respectively. The β values are -0.197 ± 0.071 (IACDM1), $0.0003 \pm$

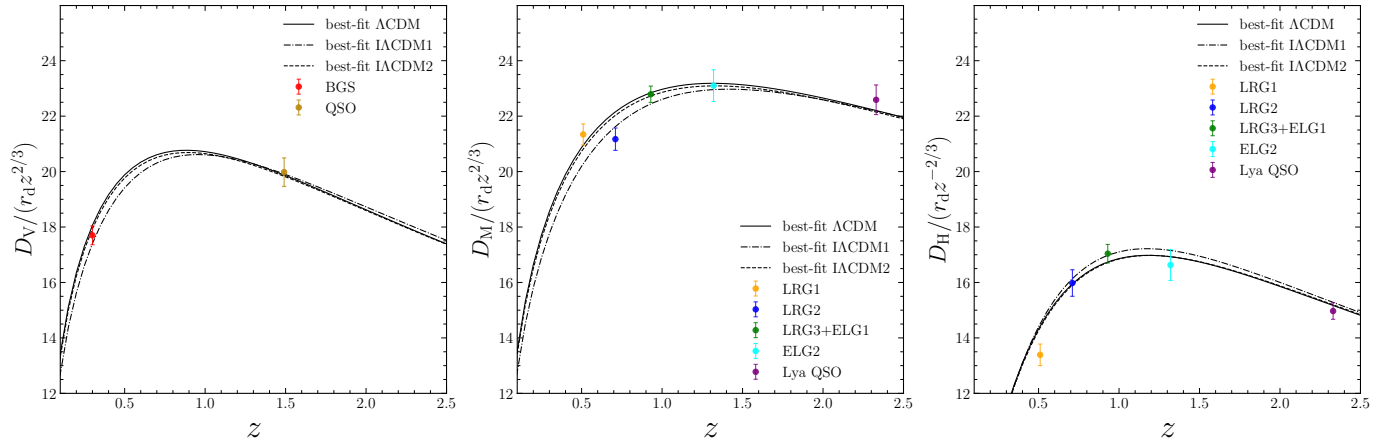


FIG. 4. Best-fit predictions for distance-redshift relations for Λ CDM (solid line), IACDM1 (dot-dashed line), and IACDM2 (dashed line) obtained from the analysis of CMB+DESI data. For visual clarity and to compress the dynamic range of the plot, we applied an arbitrary scaling. The error bars represent $\pm 1\sigma$ uncertainties.

0.0011 (IACDM2), -0.40 ± 0.13 (IACDM3), and -0.067 ± 0.038 (IACDM4) when the CMB+DESI+DESY5 data are employed. We find that β is closer to zero compared to the result obtained from CMB+DESI, which further demonstrates no interaction between dark energy and cold dark matter in the IACDM2 model. In other IDE models, it is indicated that there is an interaction where dark energy decays into cold dark matter. In particular, the deviations of β from 0 for the IACDM1 and IACDM3 models reach significance levels of 2.7σ and 3σ , respectively. For the IACDM4 model, there is still a suggestion of a deviation of β from 0 (just above 1σ), although with significantly lower statistical significance. Overall, these IDE models with $Q \propto \rho_{de}$ are more inclined to support the presence of interaction compared to those with $Q \propto \rho_c$.

In order to better understand the role played by DESI data in IDE models, we compare the theoretical distance predictions of Λ CDM and two typical IDE models (IACDM1 and IACDM2) against the observed cosmic distances in Fig. 4. Due to the relatively weak constraints provided by DESI alone, we combine DESI with CMB for our study. We analyze and compare the best-fit predictions from CMB+DESI for three different types of (rescaled) distances, including the angle-averaged distance (D_V), the transverse comoving distance (D_M), and the Hubble horizon (D_H) derived from DESI BAO measurements. Foremost, we observe that the theoretical distance predictions of the Λ CDM and IACDM2 models are largely consistent, indicating that the IACDM2 model is largely compatible with the null hypothesis, i.e., the Λ CDM model. Conversely, the theoretical distance predictions of the Λ CDM and IACDM1 models exhibit some deviations, indirectly suggesting the presence of interactions in IACDM1. Moreover, we can see that the two data points deviating from the theoretical distance predictions of the Λ CDM and IACDM2 models are the measurements of $D_M/(r_d z^{2/3})$ at $z = 0.71$ and $D_H/(r_d z^{-2/3})$

at $z = 0.51$. Interestingly, while the point $D_H/(r_d z^{-2/3})$ at $z = 0.51$ deviates from the theoretical predictions of the IACDM1 model, IACDM1 demonstrates greater success than the Λ CDM model in explaining $D_M/(r_d z^{2/3})$ at $z = 0.71$. Overall, apart from the $D_M/(r_d z^{2/3})$ and $D_H/(r_d z^{-2/3})$ at $z = 0.51$, all other BAO measurements align closely with the best-fit predictions of the IACDM1 model.

Finally, we compare the IDE models based on their fittings to the current observational data using the Akaike information criterion (AIC) [113], where $AIC \equiv \chi^2_{\min} + 2k$ and k represent the number of free parameters. In order to show the differences of AIC values between the Λ CDM and IDE models more clearly, we set the ΔAIC value of the Λ CDM model to be zero, and list the values of $\Delta AIC = \Delta \chi^2 + 2\Delta k$ in Table II, with $\Delta \chi^2 = \chi^2_{\min, \text{IDE}} - \chi^2_{\min, \Lambda\text{CDM}}$ and $\Delta k = k_{\text{IDE}} - k_{\Lambda\text{CDM}} = 1$. A model with a lower value of ΔAIC is deemed to be more supported by the observational data.

When the CMB+DESI+DESY5 data are employed to constrain the IDE models, the ΔAIC values are -2.627 (IACDM1), 1.319 (IACDM2), -4.134 (IACDM3), and -0.089 (IACDM4). The IACDM2 model, which has a slightly higher ΔAIC than the Λ CDM model, indicates that its increased model complexity is not statistically supported when fitting the CMB+DESI+DESY5 data. Other IDE models have lower ΔAIC values than the Λ CDM model, with IACDM4 model being only marginally lower. In general, the current observational data show a preference for IDE models where $Q \propto \rho_{de}$ over those where $Q \propto \rho_c$. Especially for the IACDM3 model ($Q = \beta H_0 \rho_{de}$), its ΔAIC value is significantly lower than that of the Λ CDM model, and we can conclude that this model has more advantages than the Λ CDM model.

IV. CONCLUSION

In this work, our aim is to determine whether there is an interaction between dark energy and dark matter and to identify which IDE model is more supported by the current observational data. We use DESI, CMB, and DESY5 data to constrain the IDE models. Four phenomenological IDE models are considered, i.e., IACDM1 ($Q = \beta H \rho_{de}$), IACDM2 ($Q = \beta H \rho_c$), IACDM3 ($Q = \beta H_0 \rho_{de}$), and IACDM4 ($Q = \beta H_0 \rho_c$).

We find that using CMB data alone cannot provide strong constraints on IDE models due to the degeneracy among parameters. When DESI data are added, the central value of β increases as the central value of H_0 increases, because β is positively correlated with H_0 . Specifically, the IACDM1 model with $\beta = 0.29 \pm 0.18$ provides supporting evidence for an interaction, and indicates a deviation from the standard Λ CDM model. Additionally, the best-fit predictions of the IACDM1 model align closely with the majority of BAO measurements and demonstrate greater success than the Λ CDM model in explaining $D_M/(r_d z^{2/3})$ at $z = 0.71$. When combining DESI, CMB, and DESY5 data, the constraints on cosmological parameters can be significantly improved because this combination effectively breaks the degeneracies among these parameters. Furthermore, we find that β is very close to zero, indicating no interaction between dark energy and cold dark matter in the IACDM2 model. Other IDE models suggest that there is an interaction where dark energy decays into cold dark matter. In particular, significant deviations from Λ CDM are ob-

served for the IACDM1 and IACDM3 models. Generally, IDE models with $Q \propto \rho_{de}$ support the existence of the interaction, while those with $Q \propto \rho_c$ depend on the form of the proportionality coefficient Γ to determine whether the interaction exists.

We use current observational data, including DESI, CMB, and DESY5 data, to calculate the AIC values for the four forms of IDE models. We find that the AIC values for the IACDM1 and IACDM3 models are significantly lower compared to Λ CDM and other IDE models, especially for the IACDM3 model ($Q = \beta H_0 \rho_{de}$) with $\Delta\text{AIC} = -4.134$. We can conclude that the current observational data show a preference for IDE models where $Q \propto \rho_{de}$, and the IACDM3 model has more advantages than the Λ CDM model in terms of fitting the observational data. In the coming years, the full DESI dataset combined with CMB and supernova datasets will contribute to a better understanding of the nature of dark energy. Therefore, pursuing this research is worthwhile, as future investigations may provide the necessary data to reassess this issue.

ACKNOWLEDGMENTS

We thank Yun-He Li, Yue Shao, Ji-Guo Zhang, and Bo Wang for helpful discussions. This work was supported by the National SKA Program of China (Grants Nos. 2022SKA0110200 and 2022SKA0110203), the National Natural Science Foundation of China (Grants Nos. 11975072, 11875102, 11835009, and 12305068), the National 111 Project (Grant No. B16009), and the China Scholarship Council.

-
- [1] A. G. Riess *et al.* (Supernova Search Team), *Astron. J.* **116**, 1009 (1998), arXiv:astro-ph/9805201.
 - [2] S. Perlmutter *et al.* (Supernova Cosmology Project), *Astrophys. J.* **517**, 565 (1999), arXiv:astro-ph/9812133.
 - [3] D. N. Spergel *et al.* (WMAP), *Astrophys. J. Suppl.* **148**, 175 (2003), arXiv:astro-ph/0302209.
 - [4] C. L. Bennett *et al.* (WMAP), *Astrophys. J. Suppl.* **148**, 1 (2003), arXiv:astro-ph/0302207.
 - [5] N. Aghanim *et al.* (Planck), *Astron. Astrophys.* **641**, A6 (2020), [Erratum: *Astron. Astrophys.* 652, C4 (2021)], arXiv:1807.06209 [astro-ph.CO].
 - [6] D. J. Eisenstein *et al.* (SDSS), *Astrophys. J.* **633**, 560 (2005), arXiv:astro-ph/0501171.
 - [7] S. Alam *et al.* (BOSS), *Mon. Not. Roy. Astron. Soc.* **470**, 2617 (2017), arXiv:1607.03155 [astro-ph.CO].
 - [8] S. Alam *et al.* (eBOSS), *Phys. Rev. D* **103**, 083533 (2021), arXiv:2007.08991 [astro-ph.CO].
 - [9] A. G. Riess *et al.*, *Astrophys. J. Lett.* **934**, L7 (2022), arXiv:2112.04510 [astro-ph.CO].
 - [10] L. Verde, T. Treu, and A. G. Riess, *Nature Astron.* **3**, 891 (2019), arXiv:1907.10625 [astro-ph.CO].
 - [11] A. G. Riess, *Nature Rev. Phys.* **2**, 10 (2019), arXiv:2001.03624 [astro-ph.CO].
 - [12] M. Li, X.-D. Li, Y.-Z. Ma, X. Zhang, and Z. Zhang, *JCAP* **09**, 021 (2013), arXiv:1305.5302 [astro-ph.CO].
 - [13] J.-F. Zhang, Y.-H. Li, and X. Zhang, *Phys. Lett. B* **740**, 359 (2015), arXiv:1403.7028 [astro-ph.CO].
 - [14] L. Feng, J.-F. Zhang, and X. Zhang, *Eur. Phys. J. C* **77**, 418 (2017), arXiv:1703.04884 [astro-ph.CO].
 - [15] M.-M. Zhao, D.-Z. He, J.-F. Zhang, and X. Zhang, *Phys. Rev. D* **96**, 043520 (2017), arXiv:1703.08456 [astro-ph.CO].
 - [16] R.-Y. Guo, J.-F. Zhang, and X. Zhang, *JCAP* **02**, 054 (2019), arXiv:1809.02340 [astro-ph.CO].
 - [17] R.-Y. Guo, J.-F. Zhang, and X. Zhang, *Sci. China Phys. Mech. Astron.* **63**, 290406 (2020), arXiv:1910.13944 [astro-ph.CO].
 - [18] L.-Y. Gao, Z.-W. Zhao, S.-S. Xue, and X. Zhang, *JCAP* **07**, 005 (2021), arXiv:2101.10714 [astro-ph.CO].
 - [19] E. Di Valentino, O. Mena, S. Pan, L. Visinelli, W. Yang, A. Melchiorri, D. F. Mota, A. G. Riess, and J. Silk, *Class. Quant. Grav.* **38**, 153001 (2021), arXiv:2103.01183 [astro-ph.CO].
 - [20] R.-G. Cai, Z.-K. Guo, L. Li, S.-J. Wang, and W.-W. Yu, *Phys. Rev. D* **103**, 121302 (2021), arXiv:2102.02020 [astro-ph.CO].

- [21] M. Kamionkowski and A. G. Riess, *Ann. Rev. Nucl. Part. Sci.* **73**, 153 (2023), arXiv:2211.04492 [astro-ph.CO].
- [22] L.-Y. Gao, S.-S. Xue, and X. Zhang, *Chin. Phys. C* **48**, 051001 (2024), arXiv:2212.13146 [astro-ph.CO].
- [23] G. P. Lynch, L. Knox, and J. Chluba, (2024), arXiv:2406.10202 [astro-ph.CO].
- [24] W. Zhao, C. Van Den Broeck, D. Baskaran, and T. G. F. Li, *Phys. Rev. D* **83**, 023005 (2011), arXiv:1009.0206 [astro-ph.CO].
- [25] R.-G. Cai, T.-B. Liu, X.-W. Liu, S.-J. Wang, and T. Yang, *Phys. Rev. D* **97**, 103005 (2018), arXiv:1712.00952 [astro-ph.CO].
- [26] M. Du, W. Yang, L. Xu, S. Pan, and D. F. Mota, *Phys. Rev. D* **100**, 043535 (2019), arXiv:1812.01440 [astro-ph.CO].
- [27] X. Zhang, *Sci. China Phys. Mech. Astron.* **62**, 110431 (2019), arXiv:1905.11122 [astro-ph.CO].
- [28] J.-F. Zhang, M. Zhang, S.-J. Jin, J.-Z. Qi, and X. Zhang, *JCAP* **09**, 068 (2019), arXiv:1907.03238 [astro-ph.CO].
- [29] H.-Y. Chen, *Phys. Rev. Lett.* **125**, 201301 (2020), arXiv:2006.02779 [astro-ph.HE].
- [30] H.-Y. Chen, P. S. Cowperthwaite, B. D. Metzger, and E. Berger, *Astrophys. J. Lett.* **908**, L4 (2021), arXiv:2011.01211 [astro-ph.CO].
- [31] L. Bian *et al.*, *Sci. China Phys. Mech. Astron.* **64**, 120401 (2021), arXiv:2106.10235 [gr-qc].
- [32] S.-J. Jin, L.-F. Wang, P.-J. Wu, J.-F. Zhang, and X. Zhang, *Phys. Rev. D* **104**, 103507 (2021), arXiv:2106.01859 [astro-ph.CO].
- [33] L.-F. Wang, S.-J. Jin, J.-F. Zhang, and X. Zhang, *Sci. China Phys. Mech. Astron.* **65**, 210411 (2022), arXiv:2101.11882 [gr-qc].
- [34] L.-F. Wang, Y. Shao, J.-F. Zhang, and X. Zhang, (2022), arXiv:2201.00607 [astro-ph.CO].
- [35] Z.-W. Zhao, J.-G. Zhang, Y. Li, J.-F. Zhang, and X. Zhang, (2022), arXiv:2212.13433 [astro-ph.CO].
- [36] S.-J. Jin, T.-N. Li, J.-F. Zhang, and X. Zhang, *JCAP* **08**, 070 (2023), arXiv:2202.11882 [gr-qc].
- [37] S.-J. Jin, R.-Q. Zhu, J.-Y. Song, T. Han, J.-F. Zhang, and X. Zhang, (2023), arXiv:2309.11900 [astro-ph.CO].
- [38] S.-J. Jin, S.-S. Xing, Y. Shao, J.-F. Zhang, and X. Zhang, *Chin. Phys. C* **47**, 065104 (2023), arXiv:2301.06722 [astro-ph.CO].
- [39] J.-G. Zhang, Z.-W. Zhao, Y. Li, J.-F. Zhang, D. Li, and X. Zhang, *Sci. China Phys. Mech. Astron.* **66**, 120412 (2023), arXiv:2307.01605 [astro-ph.CO].
- [40] J.-Y. Song, L.-F. Wang, Y. Li, Z.-W. Zhao, J.-F. Zhang, W. Zhao, and X. Zhang, *Sci. China Phys. Mech. Astron.* **67**, 230411 (2024), arXiv:2212.00531 [astro-ph.CO].
- [41] Y.-Y. Dong, J.-Y. Song, S.-J. Jin, J.-F. Zhang, and X. Zhang, (2024), arXiv:2404.18188 [astro-ph.CO].
- [42] S.-J. Jin, Y.-Z. Zhang, J.-Y. Song, J.-F. Zhang, and X. Zhang, *Sci. China Phys. Mech. Astron.* **67**, 220412 (2024), arXiv:2305.19714 [astro-ph.CO].
- [43] V. Sahni and A. A. Starobinsky, *Int. J. Mod. Phys. D* **9**, 373 (2000), arXiv:astro-ph/9904398.
- [44] R. Bean, S. M. Carroll, and M. Trodden, (2005), arXiv:astro-ph/0510059.
- [45] X. Zhang, *Phys. Lett. B* **611**, 1 (2005), arXiv:astro-ph/0503075.
- [46] J. Zhang, H. Liu, and X. Zhang, *Phys. Lett. B* **659**, 26 (2008), arXiv:0705.4145 [astro-ph].
- [47] M. Szydłowski, A. Krawiec, A. Kurek, and M. Kamionka, *Eur. Phys. J. C* **75**, 5 (2015), arXiv:0801.0638 [astro-ph].
- [48] M. Li, X.-D. Li, S. Wang, Y. Wang, and X. Zhang, *JCAP* **12**, 014 (2009), arXiv:0910.3855 [astro-ph.CO].
- [49] L. Zhang, J. Cui, J. Zhang, and X. Zhang, *Int. J. Mod. Phys. D* **19**, 21 (2010), arXiv:0911.2838 [astro-ph.CO].
- [50] Y. Li, J. Ma, J. Cui, Z. Wang, and X. Zhang, *Sci. China Phys. Mech. Astron.* **54**, 1367 (2011), arXiv:1011.6122 [astro-ph.CO].
- [51] Y.-H. Li and X. Zhang, *Eur. Phys. J. C* **71**, 1700 (2011), arXiv:1103.3185 [astro-ph.CO].
- [52] T.-F. Fu, J.-F. Zhang, J.-Q. Chen, and X. Zhang, *Eur. Phys. J. C* **72**, 1932 (2012), arXiv:1112.2350 [astro-ph.CO].
- [53] Z. Zhang, S. Li, X.-D. Li, X. Zhang, and M. Li, *JCAP* **06**, 009 (2012), arXiv:1204.6135 [astro-ph.CO].
- [54] J.-L. Cui, L. Yin, L.-F. Wang, Y.-H. Li, and X. Zhang, *JCAP* **09**, 024 (2015), arXiv:1503.08948 [astro-ph.CO].
- [55] X. Zhang, *Sci. China Phys. Mech. Astron.* **60**, 050431 (2017), arXiv:1702.04564 [astro-ph.CO].
- [56] H.-L. Li, D.-Z. He, J.-F. Zhang, and X. Zhang, *JCAP* **06**, 038 (2020), arXiv:1908.03098 [astro-ph.CO].
- [57] E. Di Valentino, A. Melchiorri, O. Mena, and S. Vagnozzi, *Phys. Dark Univ.* **30**, 100666 (2020), arXiv:1908.04281 [astro-ph.CO].
- [58] L. Feng, D.-Z. He, H.-L. Li, J.-F. Zhang, and X. Zhang, *Sci. China Phys. Mech. Astron.* **63**, 290404 (2020), arXiv:1910.03872 [astro-ph.CO].
- [59] M. Zhang, B. Wang, P.-J. Wu, J.-Z. Qi, Y. Xu, J.-F. Zhang, and X. Zhang, *Astrophys. J.* **918**, 56 (2021), arXiv:2102.03979 [astro-ph.CO].
- [60] L.-F. Wang, J.-H. Zhang, D.-Z. He, J.-F. Zhang, and X. Zhang, *Mon. Not. Roy. Astron. Soc.* **514**, 1433 (2022), arXiv:2102.09331 [astro-ph.CO].
- [61] S.-J. Jin, R.-Q. Zhu, L.-F. Wang, H.-L. Li, J.-F. Zhang, and X. Zhang, *Commun. Theor. Phys.* **74**, 105404 (2022), arXiv:2204.04689 [astro-ph.CO].
- [62] R. C. Nunes, S. Vagnozzi, S. Kumar, E. Di Valentino, and O. Mena, *Phys. Rev. D* **105**, 123506 (2022), arXiv:2203.08093 [astro-ph.CO].
- [63] Z.-W. Zhao, L.-F. Wang, J.-G. Zhang, J.-F. Zhang, and X. Zhang, *JCAP* **04**, 022 (2023), arXiv:2210.07162 [astro-ph.CO].
- [64] M. Forconi, W. Giarè, O. Mena, Ruchika, E. Di Valentino, A. Melchiorri, and R. C. Nunes, *JCAP* **05**, 097 (2024), arXiv:2312.11074 [astro-ph.CO].
- [65] T.-N. Li, S.-J. Jin, H.-L. Li, J.-F. Zhang, and X. Zhang, *Astrophys. J.* **963**, 52 (2024), arXiv:2310.15879 [astro-ph.CO].
- [66] T. Han, S.-J. Jin, J.-F. Zhang, and X. Zhang, (2023), arXiv:2309.14965 [astro-ph.CO].
- [67] S. Halder, J. de Haro, T. Saha, and S. Pan, *Phys. Rev. D* **109**, 083522 (2024), arXiv:2403.01397 [gr-qc].
- [68] D. Benisty, S. Pan, D. Staicova, E. Di Valentino, and R. C. Nunes, (2024), arXiv:2403.00056 [astro-ph.CO].
- [69] W. Yang, A. Mukherjee, E. Di Valentino, and S. Pan, *Phys. Rev. D* **98**, 123527 (2018), arXiv:1809.06883 [astro-ph.CO].
- [70] S. Vagnozzi, *Phys. Rev. D* **102**, 023518 (2020), arXiv:1907.07569 [astro-ph.CO].
- [71] D. Comelli, M. Pietroni, and A. Riotto, *Phys. Lett. B* **571**, 115 (2003), arXiv:hep-ph/0302080.

- [72] R.-G. Cai and A. Wang, *JCAP* **03**, 002 (2005), arXiv:hep-th/0411025.
- [73] X. Zhang, *Mod. Phys. Lett. A* **20**, 2575 (2005), arXiv:astro-ph/0503072.
- [74] A. G. Adame *et al.* (DESI), (2024), arXiv:2404.03000 [astro-ph.CO].
- [75] A. G. Adame *et al.* (DESI), (2024), arXiv:2404.03001 [astro-ph.CO].
- [76] A. G. Adame *et al.* (DESI), (2024), arXiv:2404.03002 [astro-ph.CO].
- [77] C.-G. Park, J. de Cruz Perez, and B. Ratra, (2024), arXiv:2405.00502 [astro-ph.CO].
- [78] R. Calderon *et al.*, (2024), arXiv:2405.04216 [astro-ph.CO].
- [79] Z. Wang, S. Lin, Z. Ding, and B. Hu, (2024), arXiv:2405.02168 [astro-ph.CO].
- [80] C. Escamilla-Rivera and R. Sandoval-Orozco, (2024), arXiv:2405.00608 [astro-ph.CO].
- [81] E. Di Valentino, S. Gariazzo, and O. Mena, (2024), arXiv:2404.19322 [astro-ph.CO].
- [82] Y. Yang, X. Ren, Q. Wang, Z. Lu, D. Zhang, Y.-F. Cai, and E. N. Saridakis, (2024), arXiv:2404.19437 [astro-ph.CO].
- [83] H. Wang and Y.-S. Piao, (2024), arXiv:2404.18579 [astro-ph.CO].
- [84] A. Gomez-Valent and J. Sola Peracaula, (2024), arXiv:2404.18845 [astro-ph.CO].
- [85] I. J. Allali, D. Aloni, and N. Schöneberg, (2024), arXiv:2404.16822 [astro-ph.CO].
- [86] F. J. Qu, K. M. Surrao, B. Bolliet, J. C. Hill, B. D. Sherwin, and H. T. Jense, (2024), arXiv:2404.16805 [astro-ph.CO].
- [87] D. Wang, (2024), arXiv:2404.13833 [astro-ph.CO].
- [88] E. O. Colgáin, M. G. Dainotti, S. Capozziello, S. Pourojaghi, M. M. Sheikh-Jabbari, and D. Stojkovic, (2024), arXiv:2404.08633 [astro-ph.CO].
- [89] M. Cortês and A. R. Liddle, (2024), arXiv:2404.08056 [astro-ph.CO].
- [90] D. Wang, (2024), arXiv:2404.06796 [astro-ph.CO].
- [91] W. Giarè, M. A. Sabogal, R. C. Nunes, and E. Di Valentino, (2024), arXiv:2404.15232 [astro-ph.CO].
- [92] L. Amendola, *Phys. Rev. D* **60**, 043501 (1999), arXiv:astro-ph/9904120.
- [93] A. P. Billyard and A. A. Coley, *Phys. Rev. D* **61**, 083503 (2000), arXiv:astro-ph/9908224.
- [94] E. Majerotto, J. Valiviita, and R. Maartens, *Nucl. Phys. B Proc. Suppl.* **194**, 260 (2009).
- [95] T. Clemson, K. Koyama, G.-B. Zhao, R. Maartens, and J. Valiviita, *Phys. Rev. D* **85**, 043007 (2012), arXiv:1109.6234 [astro-ph.CO].
- [96] W. Fang, W. Hu, and A. Lewis, *Phys. Rev. D* **78**, 087303 (2008), arXiv:0808.3125 [astro-ph].
- [97] W. Hu, *Phys. Rev. D* **77**, 103524 (2008), arXiv:0801.2433 [astro-ph].
- [98] Y.-H. Li, J.-F. Zhang, and X. Zhang, *Phys. Rev. D* **90**, 063005 (2014), arXiv:1404.5220 [astro-ph.CO].
- [99] Y.-H. Li, J.-F. Zhang, and X. Zhang, *Phys. Rev. D* **90**, 123007 (2014), arXiv:1409.7205 [astro-ph.CO].
- [100] Y.-H. Li, J.-F. Zhang, and X. Zhang, *Phys. Rev. D* **93**, 023002 (2016), arXiv:1506.06349 [astro-ph.CO].
- [101] Y.-H. Li and X. Zhang, *JCAP* **09**, 046 (2023), arXiv:2306.01593 [astro-ph.CO].
- [102] L. Feng, Y.-H. Li, F. Yu, J.-F. Zhang, and X. Zhang, *Eur. Phys. J. C* **78**, 865 (2018), arXiv:1807.03022 [astro-ph.CO].
- [103] A. Lewis and S. Bridle, *Phys. Rev. D* **66**, 103511 (2002), arXiv:astro-ph/0205436.
- [104] A. Lewis, *Phys. Rev. D* **87**, 103529 (2013), arXiv:1304.4473 [astro-ph.CO].
- [105] A. Gelman and D. B. Rubin, *Statist. Sci.* **7**, 457 (1992).
- [106] A. Lewis, (2019), arXiv:1910.13970 [astro-ph.IM].
- [107] N. Aghanim *et al.* (Planck), *Astron. Astrophys.* **641**, A1 (2020), arXiv:1807.06205 [astro-ph.CO].
- [108] J. Carron, M. Mirmelstein, and A. Lewis, *JCAP* **09**, 039 (2022), arXiv:2206.07773 [astro-ph.CO].
- [109] D. H. Weinberg, M. J. Mortonson, D. J. Eisenstein, C. Hirata, A. G. Riess, and E. Rozo, *Phys. Rept.* **530**, 87 (2013), arXiv:1201.2434 [astro-ph.CO].
- [110] P.-J. Wu and X. Zhang, *JCAP* **01**, 060 (2022), arXiv:2108.03552 [astro-ph.CO].
- [111] P.-J. Wu, Y. Li, J.-F. Zhang, and X. Zhang, *Sci. China Phys. Mech. Astron.* **66**, 270413 (2023), arXiv:2212.07681 [astro-ph.CO].
- [112] T. M. C. Abbott *et al.* (DES), (2024), arXiv:2401.02929 [astro-ph.CO].
- [113] H. Akaike, *IEEE Trans. Automatic Control* **19**, 716 (1974).